

# **Tetragonal Allotrope of Group 14 Elements**

## **Supporting Information**

Zhisheng Zhao,<sup>†</sup> Fei Tian,<sup>‡</sup> Xiao Dong,<sup>‡</sup> Quan Li,<sup>§</sup> Qianqian Wang,<sup>†</sup> Hui Wang,<sup>§</sup> Xin Zhong,<sup>§</sup> Bo Xu,<sup>†</sup> Dongli Yu,<sup>†</sup> Julong He,<sup>†</sup> Hui-Tian Wang,<sup>‡</sup> Yanming Ma,<sup>§\*</sup> and Yongjun Tian<sup>†\*</sup>

<sup>†</sup>State Key Laboratory of Metastable Materials Science and Technology, Yanshan University, Qinhuangdao 066004, China

<sup>§</sup>State Key Laboratory of Superhard Materials, Jilin University, Changchun 130012, China

<sup>‡</sup>School of Physics and MOE Key Laboratory of Weak-Light Nonlinear Photonics, Nankai University, Tianjin 300071, China

\* [mym@jlu.edu.cn](mailto:mym@jlu.edu.cn); [fhcl@ysu.edu.cn](mailto:fhcl@ysu.edu.cn)

## Computational Details

Our crystal structure predictions for C, Si, and Ge through CALYPSO code<sup>1,2</sup> were performed using simulation cell sizes of 2-30 atoms at pressures ranging from 0 to 20 GPa. In a typical CALYPSO run, each generation contains 30 structures, and the first generation was produced randomly, and 60% of the low-enthalpy structures of each generation were used to produce the next generation. Usually, the structure searching simulation was stopped after 600~900 structures generated (20~30 generations). All structures generated during structure search, were locally optimized using the density functional theory (DFT) within the local density approximation (LDA) and ultrasoft pseudopotentials, as implemented in the Vienna Ab-initio Simulation Package (VASP) code.<sup>3</sup> The plane wave cutoff energies of 310, 180, and 200 eV were used for C, Si, and Ge, respectively, which gave well-converged total energies within 1 meV/atom over the pressure range. In the results of CALYPSO simulations, a number of low-enthalpy experimentally and theoretically known structures (e.g., graphite, diamond, nanotubes, BC8, and ST12 structures) were found. In addition, a novel tetragonal T12 structure was uncovered.

The subsequent structural optimizations and property predictions were performed using ultrasoft pseudopotentials through the Cambridge Serial Total Energy Package (CASTEP) code.<sup>4</sup> The plane wave cutoff energies of 310, 180, and 200 eV were used for C, Si, and Ge, respectively, which were same as those used in VASP code. The electron-electron exchange interaction was described using the exchange-correlation function of Ceperley and Alder, as parameterized by Perdew and Zunger (CA-PZ) of LDA.<sup>5,6</sup> A  $k$ -point spacing ( $2\pi \times 0.04 \text{ \AA}^{-1}$ ) was used to generate the  $k$ -point grid within the Monkhorst-Pack scheme.<sup>7</sup> The electronic iterations convergence was 5.0e-7 eV/atom, and the force tolerance was 0.01 eV/ $\text{\AA}$ . The phonon frequencies were calculated using the linear response theory.<sup>8,9</sup> The phase transition paths were simulated using the variable-cell nudged elastic band (VC-NEB) method.<sup>10</sup>

**Table S1.** The optimized structural data for various carbon structures proposed earlier at ambient pressure.

| Structures                     | S.G.                   | <i>a</i>   | <i>b</i>   | <i>c</i>   | $\beta$  | Atomic positions  |
|--------------------------------|------------------------|--|--|--|--|---|
| Cco-C <sub>8</sub>             | <i>Cmmm</i> (65)       | 8.661<br>8.674 <sup>11</sup><br>8.668 <sup>12</sup><br>8.813 <sup>13</sup> | 4.203<br>4.209 <sup>11</sup><br>4.207 <sup>12</sup><br>4.274 <sup>13</sup> | 2.483<br>2.487 <sup>11</sup><br>2.486 <sup>12</sup><br>2.528 <sup>13</sup> |  | 8 <i>q</i> (-1/6, -0.815, -1/2);<br>8 <i>p</i> (-0.089, -0.315, 0)  |
| <i>P</i> -carbon               | <i>Pmmn</i> (59)       | 2.483<br>2.488 <sup>14</sup><br>2.514 <sup>15</sup>                        | 4.209<br>4.216 <sup>14</sup><br>4.263 <sup>15</sup>                        | 8.650<br>8.665 <sup>14</sup><br>8.762 <sup>15</sup>                        |  | 4 <i>e</i> (0,0.818,0.464);<br>4 <i>e</i> (0.5,0.315,0.208);<br>4 <i>e</i> (0.5,0.316,-0.285);<br>4 <i>e</i> (0.5,0.812,0.041)                                |
| <i>F</i> -carbon               | <i>P2/m</i> (10)       | 4.724<br>4.723 <sup>16</sup><br>4.730 <sup>14</sup>                        | 2.496<br>2.495 <sup>16</sup><br>2.495 <sup>14</sup>                        | 4.076<br>4.076 <sup>16</sup><br>4.084 <sup>14</sup>                        | 106.03<br>106.029 <sup>16</sup><br>106.1 <sup>14</sup> | 2 <i>n</i> (2.113, 0.5, -0.6);<br>2 <i>n</i> (1.579, 0.5, -0.632);<br>2 <i>m</i> (0.535, 0, -1/6);<br>2 <i>m</i> (0.118, 0, 0.175)                            |
| <i>O</i> -carbon               | <i>Pbam</i> (55)       | 4.748<br>4.755 <sup>17</sup><br>4.775 <sup>14</sup><br>4.757 <sup>18</sup> | 7.779<br>7.786 <sup>17</sup><br>7.789 <sup>14</sup><br>7.792 <sup>18</sup> | 2.492<br>2.494 <sup>17</sup><br>2.496 <sup>14</sup><br>2.497 <sup>18</sup> |  | 4 <i>h</i> (0.107, 0.071,0.5);<br>4 <i>h</i> (0.361, 0.955, 0.5);<br>4 <i>g</i> (0.963, 0.827, 0.0);<br>4 <i>g</i> (0.309, 0.844, 0.0)                        |
| Bct-C <sub>4</sub>             | <i>I4/mmm</i><br>(139) | 4.325<br>4.322 <sup>10</sup><br>4.329 <sup>19</sup>                        |  | 2.481<br>2.478 <sup>10</sup><br>2.483 <sup>19</sup>                        |  | 8 <i>h</i> (0.18, 0.18, 0)  |
| <i>M</i> -carbon               | <i>C2/m</i> (12)       | 9.081<br>9.089 <sup>20</sup>   | 2.493<br>2.496 <sup>20</sup>   | 4.100<br>4.104 <sup>20</sup>   | 96.95<br>96.96 <sup>20</sup>                           | 4 <i>i</i> (0.443, 0.5, 0.121);<br>4 <i>i</i> (0.442, 0, 0.347);<br>4 <i>i</i> (0.286,0.5, 0.941);<br>4 <i>i</i> (0.272, 0, 0.415)                            |
| <i>W</i> -carbon               | <i>Pnma</i> (62)       | 8.970<br>8.979 <sup>21</sup>   | 2.493<br>2.496 <sup>21</sup>   | 4.107<br>4.113 <sup>21</sup>   |  | 4 <i>c</i> (0.195,0.75,0.076);<br>4 <i>c</i> (0.189,0.25,0.301);<br>4 <i>c</i> (0.521,0.25,0.091);<br>4 <i>c</i> (0.463,0.25,0.432)                           |
| <i>X</i> -carbon               | <i>C2/c</i> (15)       | 5.487<br>5.559 <sup>22</sup>   | 7.869<br>7.960 <sup>22</sup>   | 4.692<br>4.752 <sup>22</sup>   | 114.60<br>114.65 <sup>22</sup>                         | 8 <i>f</i> (0.25,0.083,0.949);<br>8 <i>f</i> (0.489,0.809,0.982);<br>8 <i>f</i> (0.247,0.913,0.801);<br>4 <i>e</i> (0,0.2,0.25);<br>4 <i>e</i> (0,0.816,0.25) |
| <i>C</i> -carbon <sup>23</sup> | <i>Cmcm</i> (63)       | 2.491<br>2.496 <sup>18</sup>   | 11.277<br>11.293 <sup>18</sup>   | 4.848<br>4.857 <sup>18</sup>   |  | 8 <i>f</i> (0,0.868,-0.482);<br>8 <i>f</i> (0,0.442,-0.421);<br>4 <i>c</i> (0,0.778,-0.25);<br>4 <i>c</i> (0,0.2,-0.25)                                       |

**Table S2.** The optimized structural data for various metastable C, Si, and Ge phases at ambient pressure.

| Phase | Structure   | S.G.                                     | <i>a</i> | <i>b</i> | Atomic positions   |
|-------|-------------|--|----------|----------|--|
| C     | Diamond     | <i>Fd-3m</i> (227)                       | 3.528    |          | $8a (0, 0, 0)$   |
|       | Lonsdaleite | <i>P63/mmc</i> (194)                     | 2.481    | 4.133    | $4f (-1/3, -2/3, -0.563)$  |
|       | BC8         | <i>Ia-3</i> (206)                        | 4.419    |          | $16c (0.094, 0.094, 0.094)$  |
|       | $C_{136}$   | <i>Fd-3m</i> (227)                       | 9.532    |          | $96g (0.942, 0.442, 0.755);$<br>$8a (1, 0.5, 1);$<br>$32e (0.909, 0.409, 0.909)$ |
|       | T12         | <i>P42/ncm</i> (138)                     | 3.388    | 6.011    | $4b (0, 1, 0.5);$<br>$8i (-0.164, 0.336, 0.357)$                                 |
| Si    | Diamond     | <i>Fd-3m</i> (227)                       | 5.468    |          | $8a (0, 0, 0)$   |
|       | Lonsdaleite | <i>P63/mmc</i> (194)                     | 3.841    | 6.360    | $4f (-1/3, -2/3, -0.563)$  |
|       | ST12        | <i>P4<sub>3</sub>2<sub>1</sub>2</i> (96) | 5.575    | 6.682    | $8b (0.164, 0.368, -0.253);$<br>$4a (0.080, 0.080, -1/2)$                        |
|       | R8          | <i>R-3</i> (148)                         | 9.281    | 5.559    | $18f (0.231, -0.035, 0.244);$<br>$6c (0, 0, 0.285)$                              |
|       | BC8         | <i>Ia-3</i> (206)                        | 6.543    |          | $16c (0.102, 0.102, 0.102)$  |
|       | $Si_{136}$  | <i>Fd-3m</i> (227)                       | 14.695   |          | $96g (0.942, 0.442, 0.755);$<br>$8a (1, 0.5, 1);$<br>$32e (0.909, 0.409, 0.909)$ |
| Ge    | T12         | <i>P42/ncm</i> (138)                     | 5.135    | 9.167    | $4b (0, 1, 0.5);$<br>$8i (-0.164, 0.336, 0.357)$                                 |
|       | Diamond     | <i>Fd-3m</i> (227)                       | 5.548    |          | $8a (0, 0, 0)$   |
|       | Lonsdaleite | <i>P63/mmc</i> (194)                     | 3.909    | 6.457    | $4f (-1/3, -2/3, -0.563)$  |
|       | R8          | <i>R-3</i> (148)                         | 9.610    | 5.726    | $18f (0.230, -0.037, 0.238);$<br>$6c (0, 0, 0.284)$                              |
|       | ST12        | <i>P4<sub>3</sub>2<sub>1</sub>2</i> (96) | 5.790    | 6.799    | $8b (0.172, 0.370, -0.244);$<br>$4a (0.088, 0.088, -1/2)$                        |
|       | BC8         | <i>Ia-3</i> (206)                        | 6.764    |          | $16c (0.102, 0.102, 0.102)$  |
|       | $Ge_{136}$  | <i>Fd-3m</i> (227)                       | 14.932   |          | $96g (0.942, 0.442, 0.755);$<br>$8a (1, 0.5, 1);$<br>$32e (0.909, 0.409, 0.909)$ |
|       | T12         | <i>P42/ncm</i> (138)                     | 5.292    | 9.346    | $4b (0, 1, 0.5);$<br>$8i (-0.164, 0.336, 0.357)$                                 |

**Table S3.** The calculated equilibrium volume  $V_0$  ( $\text{\AA}^3/\text{atom}$ ), band gaps  $E_g$  (eV), bulk modulus  $B_0$  (GPa), shear modulus  $G_0$  (GPa), and Vickers hardness  $H_v$  (GPa) for various metastable C, Si, and Ge phases at ambient pressure, in comparison with the available experimental data in brackets.

| Phase | Structure          | $V_0$                          | $E_g$                     | $B_0$                      | $G_0$ | $H_v$                        |
|-------|--------------------|--------------------------------|---------------------------|----------------------------|-------|------------------------------|
| C     | Diamond            | 5.49 (5.67) <sup>24</sup>      | 4.20 (5.47) <sup>24</sup> | 454.6 (446) <sup>24</sup>  | 545.6 | 98.2<br>(96±5) <sup>25</sup> |
|       | Lonsdaleite        | 5.51(5.66) <sup>26</sup>       | 3.05                      | 454.5                      | 551.0 | 96.9                         |
|       | BC8                | 5.39                           | 2.35                      | 419.6                      | 557.6 | 93.2                         |
|       | $\text{C}_{136}$   | 6.37                           | 3.60                      | 381.9                      | 435.9 | 87.9                         |
|       | Cco-C <sub>8</sub> | 5.65 (5.56) <sup>27</sup>      | 3.09                      | 433.4 (447) <sup>27</sup>  | 486.9 | 95.8                         |
|       | T12                | 5.75                           | 3.59                      | 424.8                      | 479.3 | 94.0                         |
| Si    | Diamond            | 20.45 (20.02) <sup>26</sup>    | 0.55 (1.11) <sup>28</sup> | 87.9 (99) <sup>29</sup>    | 62.9  | 13.7 (13) <sup>30</sup>      |
|       | Lonsdaleite        | 20.33 (20.13) <sup>26</sup>    | 0.36                      | 79.1                       | 61.4  | 13.8                         |
|       | ST12               | 17.31                          | 1.05                      | 69.7                       | 49.8  | 15.6                         |
|       | R8                 | 17.28                          | 0.16                      | 83.7                       | 66.0  | 15.7                         |
|       | BC8                | 17.51 (18.30) <sup>31</sup>    | metallic                  | 90.5                       | 67.9  | 9.9                          |
|       | $\text{Si}_{136}$  | 23.30 (23.01) <sup>32</sup>    | 1.25 (1.9) <sup>33</sup>  | 68.6 (90) <sup>32</sup>    | 47.2  | 12.5                         |
|       | T12                | 20.15                          | 0.66                      | 88.3                       | 50.5  | 14.3                         |
| Ge    | Diamond            | 21.35 (22.65) <sup>26</sup>    | 0.34 (0.67) <sup>28</sup> | 78.0 (74.37) <sup>34</sup> | 56.9  | 12.8 (10) <sup>30</sup>      |
|       | Lonsdaleite        | 21.36 (22.31) <sup>26</sup>    | semimetallic              | 76.1                       | 52.2  | 11.5                         |
|       | R8                 | 19.08 (20.58) <sup>35</sup>    | metallic                  | 73.4 (73) <sup>35</sup>    | 48.9  | 8.3                          |
|       | ST12               | 19.00 (20.47) <sup>36</sup>    | 0.75 (1.5) <sup>37</sup>  | 67.3 (102) <sup>34</sup>   | 53.1  | 13.4                         |
|       | BC8                | 19.34 (20.82) <sup>36</sup>    | metallic                  | 75.1                       | 53.1  | 7.6                          |
|       | $\text{Ge}_{136}$  | 24.48 (25.88) <sup>38</sup>    | 0.84 (0.6) <sup>38</sup>  | 66.5 (76) <sup>35</sup>    | 43.2  | 11.7                         |
|       | T12                | 21.81 (21.72) <sup>39,40</sup> | 0.41                      | 72.6                       | 47.2  | 12.7                         |

**Table S4.** Comparison of the observed  $d$ -spacings ( $\text{\AA}$ ,  $d_{\text{obs}}$ ) of the experimental metastable Ge<sup>39,40</sup> and the calculated  $d$ -spacings ( $d_{\text{cal}}$ ) of the predicted T12 structure at ambient pressure.

| Index | $d_{\text{cal}}$ | $d_{\text{obs}}$ | $(d_{\text{obs}} - d_{\text{cal}}) / d_{\text{obs}}(\%)$ |
|-------|------------------|------------------|--|
| (100) | 5.292            | 5.37             | 1.5  |
| (101) | 4.605            | 4.57             | -0.8   |
| (110) | 3.742            | 3.80             | 1.5  |
| (111) | 3.474            | 3.46             | -0.4   |
| (112) | 2.921            | 2.919            | -0.1   |
| (200) | 2.646            | 2.68             | 1.3  |
| (201) | 2.546            | 2.569            | 0.9  |
| (113) | 2.394            | 2.42             | 1.1  |
| (004) | 2.337            |                  | -1.2   |
| (202) | 2.303            | 2.31             | 0.3  |
| (211) | 2.294            |                  | 0.7  |
| (104) | 2.137            | 2.13             | -0.3   |
| (212) | 2.111            |                  | 0.9  |
| (203) | 2.017            | 2                | -0.9   |
| (114) | 1.982            |                  | 0.9  |
| (220) | 1.871            | 1.858            | -0.7   |
| (221) | 1.835            |                  | 1.2  |
| (300) | 1.764            | 1.791            | 1.5  |

Note:

The electron diffraction intensities in transmission electron microscopy (TEM) observations were obtained in Refs. 39 and 40. However, it is established that electron diffraction intensities in TEM observations are strongly dependent on the thickness, crystallinity, zone axis, and electron density of the crystal plane of the sample. Moreover, the forbidden reflections are often observed due to the multidiffraction effect. Therefore, the relative electron diffraction intensities are hardly meaningful in TEM observations. It should be noted that there are more diffraction lines in the calculated structure than in the experimental observation. This might be due to the limitation of experimental resolution during measurement.

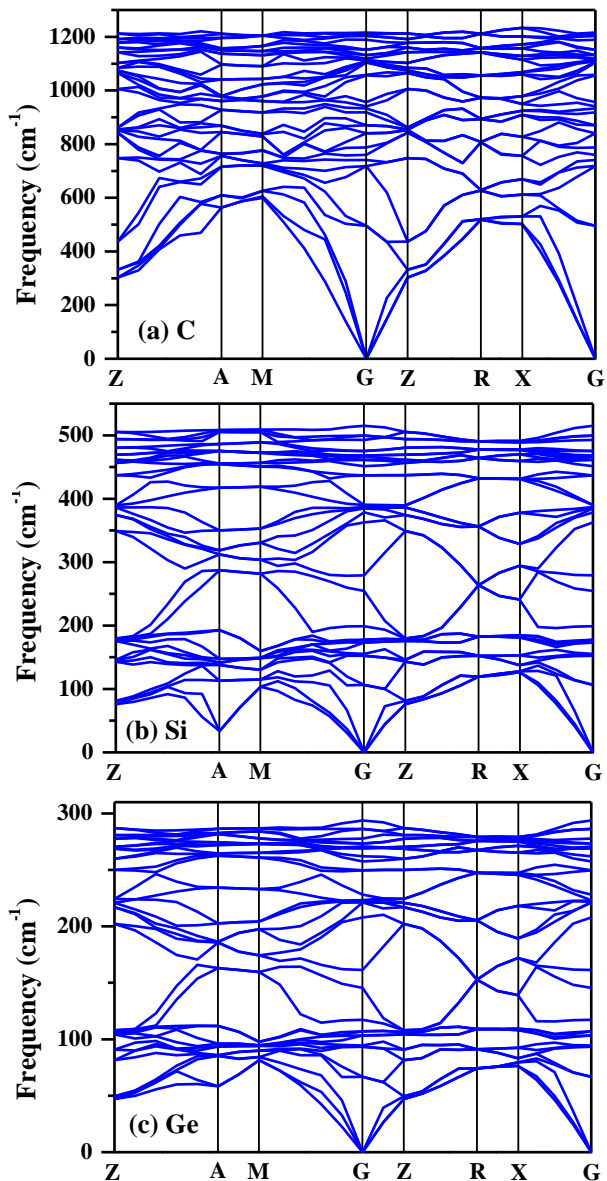


**Figure S1.** Phonon dispersion curves of T12 structured C (a), Si (b), and Ge (c) at ambient pressure.

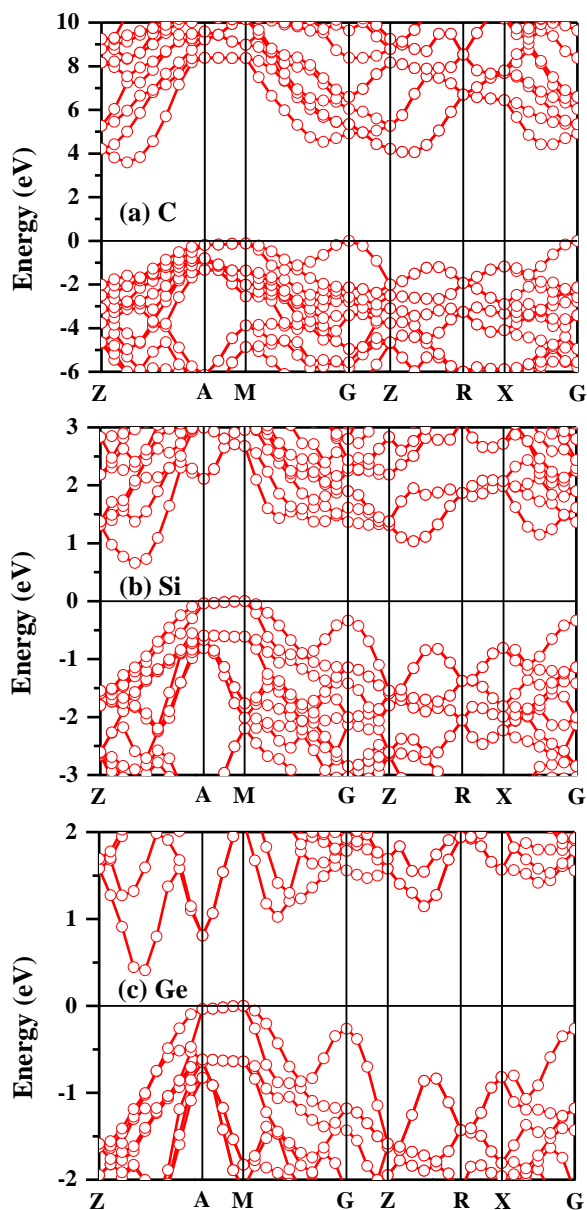


**Figure S2.** Electronic band structures of T12 structured C (a), Si (b) and Ge (c) at ambient pressure.

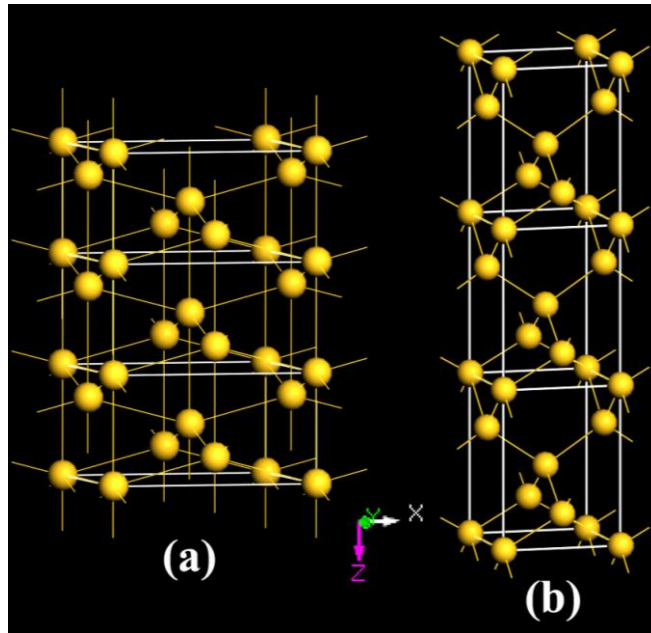


**Figure S3.** Crystal structures of  $\beta$ -Sn (a) and diamond (b) structured Si.

Note:

Diamond-Si and  $\beta$ -Sn Si have similar structures. The  $\beta$ -Sn Si becomes diamond-Si when lattice parameter  $a$  (and  $b$ ) is shortened and  $c$  is elongated to some extent. At 5 GPa, the optimized lattice parameters  $a$  and  $c$  are 4.665 and 2.589 Å for  $\beta$ -Sn Si, and 3.751 and 5.299 Å for diamond-Si respectively. The VC-NEB method successfully searched the highest saddle points of energy barrier in  $\beta$ -Sn Si $\rightarrow$ diamond-Si transition corresponding to structures of image 6 and 7 in Fig. 2d. The lattice parameters become  $a=4.5$  Å,  $b=4.188$  Å and  $c=3.533$  Å at image 6, and become  $a=4.5$  Å,  $b=4.188$  Å and  $c=3.567$  Å at image 7. After full optimization, the image 6 structure changes back to  $\beta$ -Sn Si, while the image 7 structure into diamond-Si. Our results of systematic simulations indicated that image 6 and 7 structures undoubtedly are located at the highest saddle points with lowest energy barrier of 0.227 eV/atom for the  $\beta$ -Sn Si $\rightarrow$ diamond-Si transition.

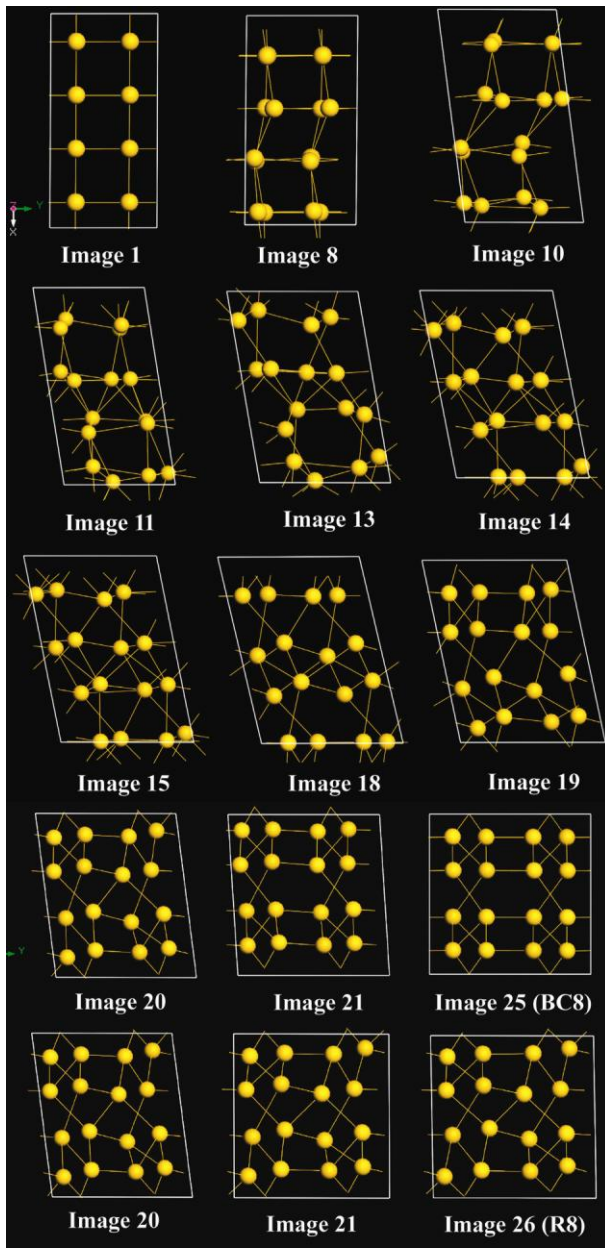


**Figure S4.** Transition paths from  $\beta$ -Sn to BC8 and R8 structured Si (Si-III and Si-XII) at 5 GPa, respectively. The structural image numbers correspond to those in Fig. 2d.

Note:

BC8- and R8-Si have the similar structures, and R8 structure can be seen as a reconfiguration formed through the bonding of one pair of unbonded atoms in parent BC8 primitive cell, so the two phases appear competitive in the phase transition after image 20 (Fig. 2d and S4), consistent with experimental observation.<sup>31</sup>

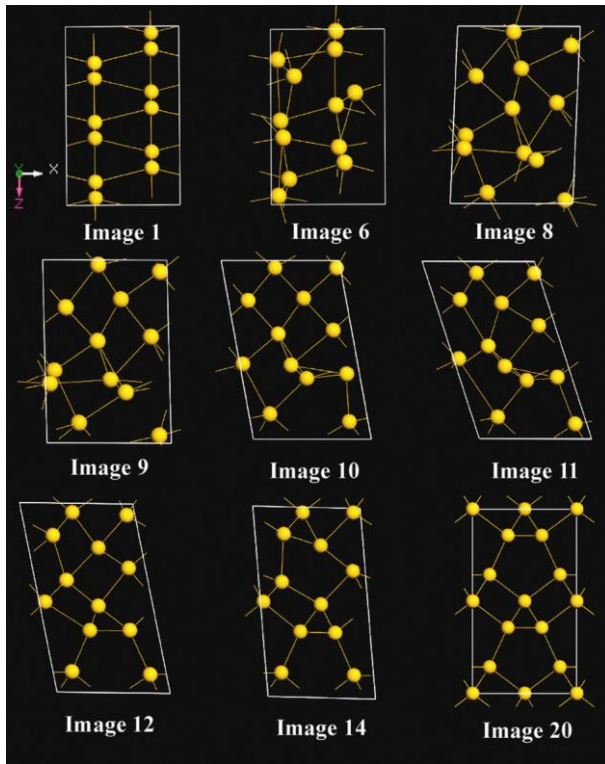


**Figure S5.** Transition paths from  $\beta$ -Sn to T12 structured Si at 5 GPa. The structural image numbers correspond to those in Fig. 2d.

## References:

- (1) Wang, Y.; Lv, J.; Zhu, L.; Ma, Y. *Phys. Rev. B* **2010**, *82*, 094116.
- (2) Wang, Y.; Lv, J.; Zhu, L.; Ma, Y. *Comput. Phys. Commun.* **2012**, *183*, 2063.
- (3) Kresse, G.; Furthmüller, J. *Phys. Rev. B* **1996**, *54*, 11169.
- (4) Clark, S. J.; Segall, M. D.; Pickard, C. J.; Hasnip, P. J.; Probert, M. I. J.; Refson, K.; Payne, M. C. *Zeitschrift für Kristallographie* **2005**, *220*, 567.
- (5) Ceperley, D. M.; Alder, B. J. *Phys. Rev. Lett.* **1980**, *45*, 566.
- (6) Perdew, J. P.; Zunger, A. *Phys. Rev. B* **1981**, *23*, 5048.
- (7) Monkhorst, H. J.; Pack, J. D. *Phys. Rev. B* **1976**, *13*, 5188.
- (8) Baroni, S.; Giannozzi, P.; Testa, A. *Phys. Rev. Lett.* **1987**, *58*, 1861.
- (9) Giannozzi, P.; de Gironcoli, S.; Pavone, P.; Baroni, S. *Phys. Rev. B* **1991**, *43*, 7231.
- (10) Zhou, X.-F.; Qian, G.-R.; Dong, X.; Zhang, L.; Tian, Y.; Wang, H.-T. *Phys. Rev. B* **2010**, *82*, 134126.
- (11) Zhao, Z.; Xu, B.; Zhou, X.-F.; Wang, L.-M.; Wen, B.; He, J.; Liu, Z.; Wang, H.-T.; Tian, Y. *Phys. Rev. Lett.* **2011**, *107*, 215502.
- (12) Amsler, M.; Flores-Livas, J. A.; Lehtovaara, L.; Balima, F.; Ghasemi, S. A.; Machon, D.; Pailhès, S.; Willand, A.; Caliste, D.; Botti, S.; San Miguel, A.; Goedecker, S.; Marques, M. A. L. *Phys. Rev. Lett.* **2012**, *108*, 065501.
- (13) Selli, D.; Baburin, I. A.; Martoňák, R.; Leoni, S. *Phys. Rev. B* **2011**, *84*, 161411.

- (14) Niu, H.; Chen, X.-Q.; Wang, S.; Li, D.; Mao, W. L.; Li, Y. *Phys. Rev. Lett.* **2012**, *108*, 135501.
- (15) He, C.; Sun, L.; Zhang, C.; Peng, X.; Zhang, K.; Zhong, J. *PCCP* **2012**, *14*, 8410.
- (16) Tian, F.; Dong, X.; Zhao, Z.; He, J.; Wang, H. T. *J. Phys.: Condens. Matter* **2012**, *24*, 165504.
- (17) Wang, J.-T.; Chen, C.; Kawazoe, Y. *Phys. Rev. B* **2012**, *85*, 033410.
- (18) He, C.; Sun, L.; Zhang, C.; Peng, X.; Zhang, K.; Zhong, J. *Solid State Commun.* **2012**, DOI: <http://dx.doi.org/10.1016/j.ssc.2012.05.022>.
- (19) Umemoto, K.; Wentzcovitch, R. M.; Saito, S.; Miyake, T. *Phys. Rev. Lett.* **2010**, *104*, 125504.
- (20) Li, Q.; Ma, Y.; Oganov, A. R.; Wang, H.; Wang, H.; Xu, Y.; Cui, T.; Mao, H.-K.; Zou, G. *Phys. Rev. Lett.* **2009**, *102*, 175506.
- (21) Wang, J.-T.; Chen, C.; Kawazoe, Y. *Phys. Rev. Lett.* **2011**, *106*, 075501.
- (22) Zhu, Q.; Zeng, Q.; Oganov, A. R. *Phys. Rev. B* **2012**, *85*, 201407.
- (23) Li, D.; Bao, K.; Tian, F.; Zeng, Z.; He, Z.; Liu, B.; Cui, T. *PCCP* **2012**, *14*, 4347.
- (24) Occelli, F.; Loubeyre, P.; LeToullec, R. *Nature materials* **2003**, *2*, 151.
- (25) Gao, F.; He, J.; Wu, E.; Liu, S.; Yu, D.; Li, D.; Zhang, S.; Tian, Y. *Phys. Rev. Lett.* **2003**, *91*, 015502.
- (26) Raffy, C.; Furthmüller, J.; Bechstedt, F. *Physical Review B* **2002**, *66*, 075201.
- (27) Wang, Z.; Zhao, Y.; Tait, K.; Liao, X.; Schiferl, D.; Zha, C.; Downs, R. T.; Qian, J.; Zhu, Y.; Shen, T. *Proc. Natl. Acad. Sci. U.S.A.* **2004**, *101*, 13699.
- (28) [http://en.wikipedia.org/wiki/Band\\_Gap#cite\\_note-Streetman-5](http://en.wikipedia.org/wiki/Band_Gap#cite_note-Streetman-5).
- (29) Yin, M. T.; Cohen, M. L. *Physical Review B* **1982**, *26*, 5668.
- (30) Vandeperre, L. J.; Giuliani, F.; Lloyd, S. J.; Clegg, W. J. *Acta Materialia* **2007**, *55*, 6307.
- (31) Crain, J.; Ackland, G. J.; Maclean, J. R.; Piltz, R. O.; Hatton, P. D.; Pawley, G. S. *Phys. Rev. B* **1994**, *50*, 13043.
- (32) Ramachandran, Ganesh K; McMillan, P. F.; Deb, Sudip K; Somayazulu, Maddury; Gryko, Jan; Dong, Jianjun; Sankey, Otto F J. *Phys.: Condens. Matter* **2000**, *12*, 4013.
- (33) Gryko, J.; McMillan, P. F.; Marzke, R. F.; Ramachandran, G. K.; Patton, D.; Deb, S. K.; Sankey, O. F. *Phys. Rev. B* **2000**, *62*, R7707.
- (34) Menoni, C. S.; Hu, J. Z.; Spain, I. L. *Phys. Rev. B* **1986**, *34*, 362.
- (35) Schwarz, U.; Wosylus, A.; Böhme, B.; Baitinger, M.; Hanfland, M.; Grin, Y. *Angew. Chem. Int. Ed.* **2008**, *47*, 6790.
- (36) Nelmes, R. J.; McMahon, M. I.; Wright, N. G.; Allan, D. R.; Loveday, J. S. *Phys. Rev. B* **1993**, *48*, 9883.
- (37) Sato, S.; Nozaki, S.; Morisaki, H. *Appl. Phys. Lett.* **1998**, *72*, 2460.
- (38) Guloy, A. M.; Ramlau, R.; Tang, Z.; Schnelle, W.; Baitinger, M.; Grin, Y. *Nature* **2006**, *443*, 320.
- (39) Saito, Y. *J. Cryst. Growth* **1979**, *47*, 61.
- (40) Saito, Y.; Yatsuya, S.; Mihamata, K.; Uyeda, R. *Jpn. J. Appl. Phys.* **1978**, *17*, 291.